



Pre-TACE kurtosis of ADC_{total} derived from histogram analysis for diffusion-weighted imaging is the best independent predictor of prognosis in hepatocellular carcinoma

Li-Fang Wu¹ · Sheng-Xiang Rao² · Peng-Ju Xu² · Li Yang² · Cai-Zhong Chen² · Hao Liu² · Jian-Feng Huang² · Cai-Xia Fu³ · Alice Halim⁴ · Meng-Su Zeng²

Received: 2 February 2018 / Revised: 5 April 2018 / Accepted: 11 April 2018 / Published online: 19 June 2018

© European Society of Radiology 2018

Abstract

Purpose To determine the feasibility of pre-TACE IVIM imaging based on histogram analysis for predicting prognosis in the treatment of unresectable hepatocellular carcinoma (HCC).

Materials and methods Fifty-five patients prospectively underwent 1.5T MRI 1 week before TACE. Histogram metrics for IVIM parameters and ADCs maps between responders and non-responders with mRECIST assessment were compared. Kaplan–Meier, log-rank tests and Cox proportional hazard regression model were used to correlate variables with time to progression (TTP).

Results Mean ($p = 0.022$), median ($p = 0.043$), and 25th percentile ($p < 0.001$) of perfusion fraction (PF), mean ($p < 0.001$), median ($p < 0.001$), 25th percentile ($p < 0.001$) and 75th percentile ($p = 0.001$) of $ADC_{(0,500)}$, mean ($p = 0.005$), median ($p = 0.008$) and 25th percentile ($p = 0.039$) of ADC_{total} were higher, while skewness and kurtosis of PF ($p = 0.001$, $p = 0.005$, respectively), kurtosis of $ADC_{(0,500)}$ and ADC_{total} ($p = 0.005$, $p = 0.001$, respectively) were lower in responders compared to non-responders. Multivariable analysis demonstrated that mRECIST was associated with TTP independently, and kurtosis of ADC_{total} had the best predictive performance for disease progression.

Conclusion Pre-TACE kurtosis of ADC_{total} is the best independent predictor for TTP.

Key Points

- mRECIST was associated with TTP independently.
- Lower kurtosis and higher mean for ADCs tend to have good response.
- Pre-TACE kurtosis of ADC_{total} is the best independent predictor for TTP.

Keywords Magnetic resonance imaging · Diffusion · Hepatocellular carcinoma · Therapy · Prognosis

Abbreviations

ADC	Apparent diffusion coefficient
D_{fast}	Pseudodiffusion coefficient
D_{slow}	True diffusion coefficient
IVIM	Intravoxel incoherent motion
PF	Perfusion fraction
TACE	Transarterial chemoembolisation
TTP	Time to progression

Introduction

Transarterial chemoembolisation (TACE) is the main form of treatment for hepatocellular carcinoma (HCC) patients with multifocal or large lesions and compensated liver function

✉ Meng-Su Zeng
zeng.mengsu@zs-hospital.sh.cn

¹ Shanghai Institute of Medical Imaging, Department of Radiology, Zhongshan Hospital, Fudan University, No. 180, Fenglin Road, Xuhui District, Shanghai 200032, China

² Department of Radiology, Zhongshan Hospital, Fudan University, Shanghai Institute of Medical Imaging, No. 180, Fenglin Road, Xuhui District, Shanghai 200032, China

³ Siemens Healthcare, Siemens MR Center, Gaoxin C. Ave., 2nd, Hi-Tech Industrial Park, Shenzhen 518057, China

⁴ Fudan University, No. 130, Dongan Road, Xuhui District, Shanghai 200032, China

who are untreatable by resection [1]. Partial response was observed in 15–55% of patients who had received TACE, which showed significant delay in tumour progression including macrovascular invasion [2]. In patients with TACE failure, additional therapy may be considered. In order to decide the optimal therapeutic pretreatment option for each patient with an acceptable balance of risks and benefits, a key aspect lies in the assessment of patients via Barcelona Clinic Liver Cancer (BCLC) staging. This criterion is widely used to determine suitable treatment strategies validated by various scientific associations and research consortia [1–4]. Previous studies have focused on response evaluation with parameter changes reflecting HCC diffusion and perfusion characteristics derived from uni- or bi-exponential model of diffusion-weighted magnetic resonance imaging (DW-MRI) before and after TACE [5–7]. However, the results do not show consistent correlation between pre-TACE apparent diffusion coefficient (ADC) values of hepatic lesions and survival benefits.

A histogram is a particularly sensitive feature for pathological assessment; it provides additional parameters beyond the mean and quantitatively reflects the distribution of signal intensity throughout all tumour voxels [8], which has been widely used in the characterisation of benign versus malignant lesions in different tumours [8–12]. A biexponential model of intravoxel incoherent motion (IVIM) can noninvasively provide microcirculatory perfusion measurement in addition to diffusivity [13]. In this present study, we aimed to determine prospectively the feasibility of IVIM imaging based on histogram analysis to predict the efficacy of TACE.

Materials and methods

Patients

In this prospective study, we included 55 patients (mean age, 58 years, range, 35–83 years; 45 males and 10 females) with unresectable liver-confined HCC who were eligible for TACE between May 2014 and September 2016 under the approval of our hospital's Institutional Review Board. All patients gave their written informed consent. Subsequently, we enrolled patients according to: (1) Existence of single or multinodular HCC diagnosed independently by two experienced clinicians on the basis of typical dynamic contrast-enhanced imaging combined with alpha fetoprotein (AFP) serology, according to the American Association for the Study of Liver Diseases (AASLD) guidelines [4]. (2) Presence of pretreatment MRI, including IVIM-DWI; brain and chest computed tomography (CT) were also implemented to exclude extrahepatic metastasis. (3) BCLC stage A or B and Child-Pugh class A or B [2, 4]. Exclusion criteria consisted of the following: (1) previous oncological treatment or recurrent HCC patients within 1 year after the last treatment; (2) tumour invasion of branches and

trunk of the portal vein or hepatic veins on MRI; and (3) extrahepatic metastasis.

Transarterial chemoembolisation (TACE)

To identify all the feeding arteries of the tumour, angiography of the coeliac, hepatic, superior mesenteric, left gastric and bilateral inferior phrenic artery was performed with a 5-F RH catheter (Cook). After inserting a 2.7-F microcatheter (Renegade, Boston Scientific) into the target artery, 10–50 mg/m² of epirubicin hydrochloride (Pharmorubicin, Pfizer) was mixed with 5–20 ml of iodised oil (Lipiodol Ultrafluide, Laboratoire Guerbet) via a pumping method. The dose of iodised oil and epirubicin was determined according to the tumour size and patient's liver function. Under fluoroscopic monitoring, the mixture was infused through the microcatheter at a rate of 0.5–1 ml/min until flow in the tumour vascularity became stasis. Finally, a gelatin sponge 1–2 mm in diameter (Jingling) was used to embolise the feeding artery.

Imaging technique

All MR images were acquired on a 1.5T scanner (Magnetom Area; Siemens Healthineers) with phased-array coil 1 week before TACE (range, 1–7 days). The following sequences were used: A single-shot spin-echo planar free breathing IVIM DW imaging sequence with a bipolar DW scheme was performed in the axial view with 12 b values (0, 10, 20, 30, 40, 50, 70, 100, 200, 300, 500 and 800 s/mm²) (repetition time [TR]/echo time [TE] = 4,100/70 ms; section thickness, 6 mm; intersection gap, 1 mm; field of view [FOV] optimised to patients' body habitus, 285 × 214–308 × 380 mm; matrix, 128 × 128) with a total acquisition time of about 6–7 min. Transverse respiratory-triggered T2-weighted with fat suppression turbo spin echo sequence (TR/TE = 3,400/106 ms; slice thickness, 5 mm; intersection gap, 1 mm; FOV optimised to patients' body habitus, 285 × 214–308 × 380 mm; matrix, 168 × 320) with a total acquisition time about 3–4 min and transverse T1-weighted breath-hold in-phase and opposed-phase gradient echo (TR/TE = 6.87/4.75 [in-phase], 2.38 [opposed-phase] ms; section thickness, 4 mm; intersection gap, 1 mm; FOV optimised to patients' body habitus, 285 × 214–308 × 380 mm; matrix, 180 × 320). A T1-weighted with fat-suppressed volumetric interpolated breath-hold examination (VIBE) sequence (TR/TE = 4.36/2.00 ms; section thickness, 3 mm; no intersection gap; FOV optimised to patients' body habitus, 285 × 214–308 × 380 mm; matrix, 270 × 360) was performed before and after injection of contrast media. Arterial, portal venous and delayed phases were obtained at 20–30 s, 70–80 s and 180 s after a 0.2 ml/kg bolus injection of gadopentetate dimeglumine at a rate of 2 ml/s.

Imaging assessment

Diffusion-weighted imaging (DWI)

The acquired DWI data were post-processed using an IVIM work-in progress package (provided by Siemens Healthineers) so as to obtain the following parameters: true diffusion coefficient (D_{slow}), pseudodiffusion coefficient (D_{fast}) and perfusion fraction (PF), which were calculated using the formula $S_b/S_0 = (1 - \text{PF}) \cdot e^{(-b \cdot D_{\text{slow}})} + \text{PF} \cdot e^{(-b \cdot D_{\text{fast}})}$, where $S(b)$ is the mean signal intensity (SI) under the given b value. In addition, $\text{ADC}_{\text{total}}$ and $\text{ADC}_{(0,500)}$ were calculated using 12 b values (0, 10, 20, 30, 40, 50, 70, 100, 200, 300, 500 and 800 s/mm^2) and two b values (0, 500 s/mm^2) with monoexponential fit using the model equation $S_b = S_0 \cdot e^{-b\text{ADC}}$.

Histogram analysis

A prototype software (MR OncoTreat, Siemens Healthineers) was used for histogram analysis on a Windows personal computer. The qualitative analysis was performed by one radiologist (L.Y., with 7 years of experience) who was blinded to any other results and was initially trained before the qualitative evaluation. For histogram analysis, DICOM data including IVIM images of b value = 0 s/mm^2 , D_{slow} , D_{fast} , PF, $\text{ADC}_{(0,500)}$ and $\text{ADC}_{\text{total}}$ maps were loaded into the OncoTreat software. The largest lesion was chosen as the target lesion. The radiologist manually painted the seed points for the whole lesion as large as possible covering both the viable and necrotic portion on IVIM (b value = 0 s/mm^2) sequences from representative axial, sagittal and coronal images while avoiding large vessels, then automated co-registration of morphological images and corresponding parametric maps, and finally ran the semiautomatic 3D tumour segmentation (Figs. 1 and 2). The results of segmentation can be corrected by adjusting seed points to assure the voxel-based histogram data was generated for the entire target lesion without adjacent liver parenchyma. The following parameters were calculated: mean, median, standard deviation, skewness, kurtosis and the 25th, 75th and 90th percentiles.

Follow-up strategy

All patients were followed up with monthly abdominal DCE MRI or CT and combined chest examinations, tumour markers and biochemical liver function tests for at least 6 months. Considering cost effectiveness and inter-patient variability, a 2-month interval at most has been adopted according to the idiomatic follow-up protocol in our hospital, which also coincides with Japanese guidelines [14, 15], in the next 6 months. Thereafter follow-up is conducted every 3–6 months as necessary. Patients with documented disease progression during the follow-up underwent additional TACE and/or systemic therapy.

Reference standard

TACE response was evaluated according to the modified Response Evaluation Criteria in Solid Tumors (mRECIST) [16], for which a maximum of two enhancing lesions were chosen as target lesion if multinodular. mRECIST assessment is based on the sum of unidimensional measurements of arterially-enhancing lesions of pre-TACE MR as well as 1 month after treatment MR or CT, defining complete response (CR) as disappearance of any intra-tumoral enhancement, partial response (PR) as at least a 30% decrease from baseline; progressive disease (PD) as at least a 20% increase from baseline; and stable disease (SD) as any response that did not qualify for inclusion in other categories [2, 17]. The appearance of new lesions or extra-hepatic metastases is also considered as PD. Patients with SD and PD were classified as non-responders while CR and PR were classified as responders. Time to progression (TTP) was defined as the time between the start of treatment and PD.

Statistical analysis

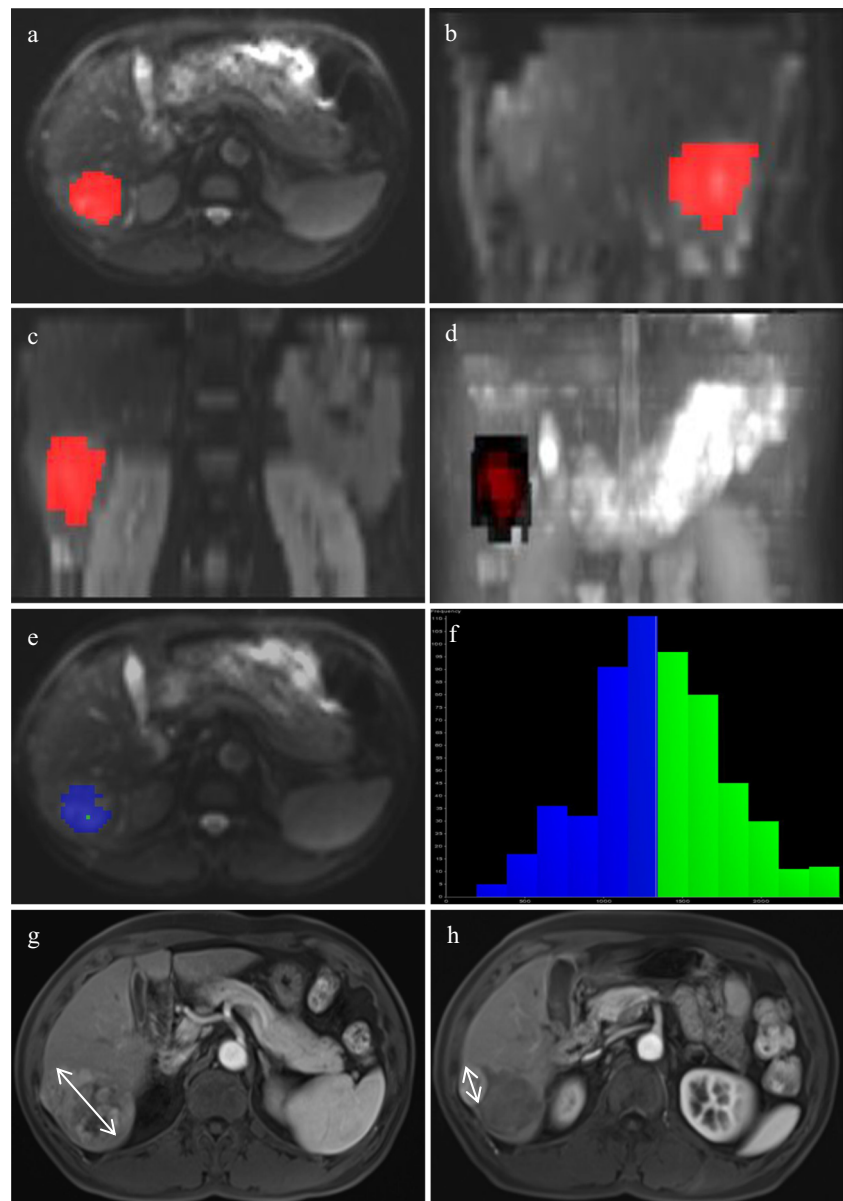
Statistical analyses were performed using SPSS (v. 20.0) and MedCalc software (MedCalc). Baseline characteristics of the patients were expressed as mean and standard deviation or count. Continuous variables were compared with Student's t -test or the Mann–Whitney U -test if not normally distributed. Categorical variables were compared using Pearson's chi-squared test or Fisher's exact test. The histogram analyses for DWI parameters were compared between responders and non-responders using Student's t -test or Mann–Whitney U -test. Additionally, ROC analyses were conducted on significant parameters to assess the ability of the imaging measures to discriminate between the responders and non-responders. Univariate analysis was performed using Kaplan–Meier and log rank tests to correlate the response variables with TTP. Multivariate analysis was performed by using Cox proportional hazard regression to determine independent factors associated with disease progression. A difference with a p -value of less than 0.05 was considered statistically significant.

Results

Patient characteristics

Patient pretreatment characteristics are listed in Table 1. There were 25 responders (2 complete responders, 23 partial responders) and 30 non-responders (18 stable disease, 12 progressions) according to mRECIST. The TTP of patients ranged from 27 days to 819 days with 14 censored data until September 2017.

Fig. 1 A partial responder with hepatocellular carcinoma (HCC) in the right lobe (segment 6) before transarterial chemoembolisation (TACE). Regions of interest were manually circumscribed on intravoxel incoherent motion (IVIM) (b value = 0 s/mm²) sequences from representative axial (a), sagittal (b) and coronal images (c). Semiautomatic 3D tumour segmentation (d). Corresponding ADC_{total} map (e). mRECIST response indicated a more than 30% decrease in the longest diameter of the enhancing tumour component between g, imaging before treatment and h, imaging 1 month after treatment (partial response). Histogram analyses of entire lesion shows low kurtosis of 2.90 and high median ADC_{total} of 1.33×10^{-3} mm²/s. The patient had a time to progression (TTP) of 263 days



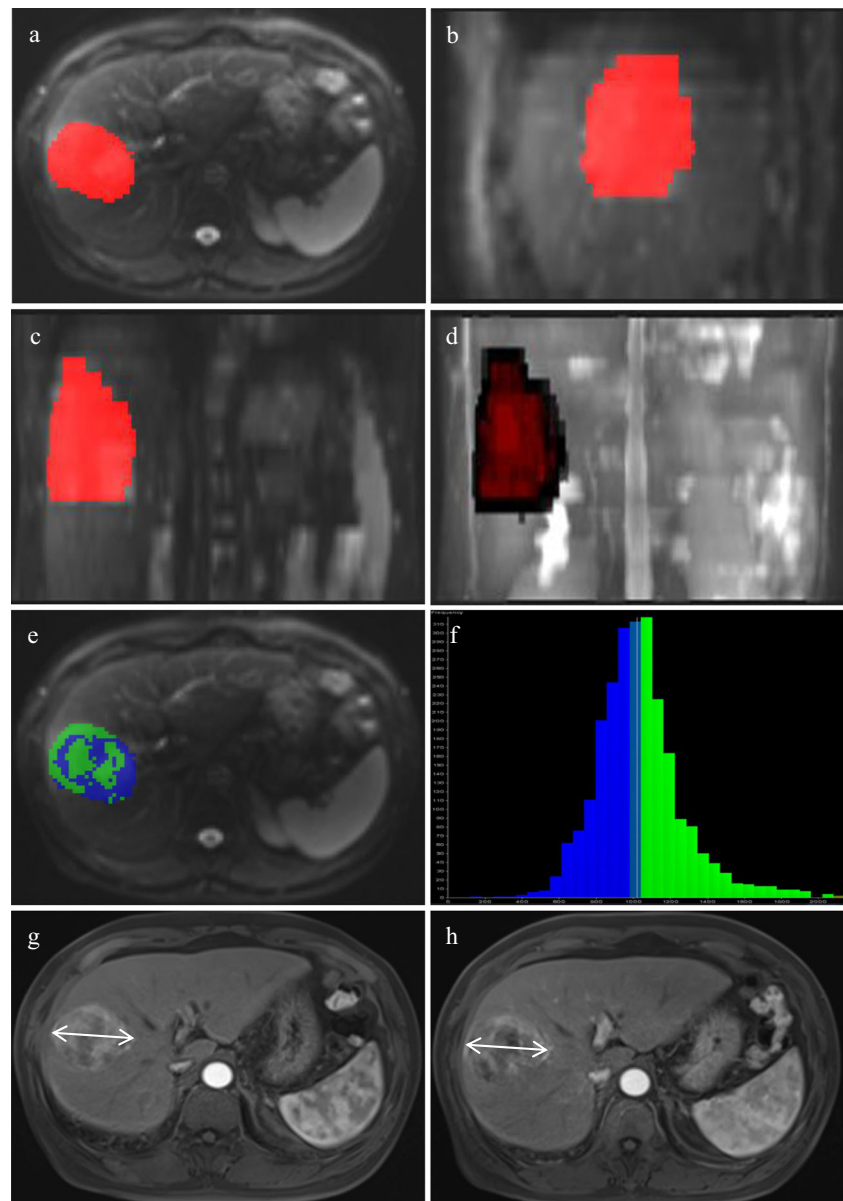
Histogram measurements

The mean values of histogram metrics (mean, median, 25th, 75th and 90th percentiles, standard deviation, skewness and kurtosis) for D_{slow} , D_{fast} , PF, $ADC_{(0,500)}$ and ADC_{total} maps are provided in Table 2. Median D_{slow} ($p = 0.045$), mean ($p = 0.022$), median ($p = 0.043$), 25th percentile ($p < 0.001$) and 75th percentile ($p = 0.031$) of PF, mean ($p < 0.001$), median ($p < 0.001$), 25th percentile ($p < 0.001$), 75th percentile ($p = 0.001$) and standard deviation ($p = 0.049$) of $ADC_{(0,500)}$, mean ($p = 0.005$), median ($p = 0.008$) and 25th percentile ($p = 0.039$) of ADC_{total} were higher, while skewness and kurtosis of PF ($p = 0.001$, $p = 0.005$, respectively), kurtosis of $ADC_{(0,500)}$ ($p = 0.005$) and kurtosis of ADC_{total} ($p = 0.001$) were lower in responders compared with non-responders.

Diagnostic performance for identifying responders and non-responders

With regard to the above-mentioned parameters that showed a significant difference in the histogram analyses between responders and non-responders (Table 2), ROC curve analyses were further performed to evaluate diagnostic performance. The optimal cut-off value, as well as corresponding AUCs, p values, sensitivities, specificities, positive predictive values (PPVs) and negative predictive values (NPVs) are shown in Table 3 and Fig. 3. The p value of median D_{slow} ($p = 0.063$), 75th percentile of PF ($p = 0.059$) and standard deviation of $ADC_{(0,500)}$ ($p = 0.061$) were > 0.05 , which meant that these parameters failed to distinguish responders from non-responders. Among the rest of the significant parameters, the best one,

Fig. 2 A non-responder of stable disease with hepatocellular carcinoma (HCC) in the right lobe (segments 5, 6, 7 and 8) before transarterial chemoembolisation (TACE). Regions of interest were manually circumscribed on intravoxel incoherent motion (IVIM) (b value = 0 s/mm^2) sequences from representative axial (**a**), sagittal (**b**) and coronal images (**c**). Semiautomatic 3D tumour segmentation (**d**). Corresponding $\text{ADC}_{\text{total}}$ map (**e**). mRECIST response shows no diameter change between **g**, imaging before treatment and **h**, imaging 1 month after treatment (stable disease). Histogram analysis of the entire lesion shows high kurtosis of 5.18 and low median $\text{ADC}_{\text{total}}$ of $1.01 \times 10^{-3} \text{ mm}^2/\text{s}$. The patient had a time to progression (TTP) of 86 days



kurtosis of $\text{ADC}_{\text{total}}$, had an AUC of 0.82, with a sensitivity of 76% and specificity of 86.7% at the optimum threshold of 4.69.

Association with time to progression (TTP)

A significant association was found between TTP and mRECIST criteria ($p < 0.001$). With regard to pretreatment clinical characteristics (Table 1) and histogram metrics that showed a significant difference between different groups (Table 3), mean PF ($p = 0.076$), median $\text{ADC}_{(0,500)}$ ($p = 0.096$) and kurtosis of $\text{ADC}_{(0,500)}$ ($p = 0.691$) failed to establish an association with TTP via univariate analysis. The result of association between the rest of the variables and TTP with univariate and multivariate analysis is shown in Table 4.

TTP was significantly higher in responders with mRECIST assessment than in non-responders ($p < 0.001$). Patients with a kurtosis value of $\text{ADC}_{\text{total}}$ below 4.69 had significantly higher TTP than those above 4.69 ($p = 0.036$) (Fig. 4).

Table 5 showed relationships between independent factors and TTP. mRECIST criteria (hazard ratio [HR] = 642.088) and 75th percentile of $\text{ADC}_{(0,500)}$ (HR = 5.742) demonstrated positive correlations with TTP, while kurtosis of $\text{ADC}_{\text{total}}$ (HR = 0.266) showed negative correlations.

Discussion

Our study showed that histogram-derived parameters for PF, $\text{ADC}_{(0,500)}$ and $\text{ADC}_{\text{total}}$ maps were useful for discrimination

Table 1 Patient baseline characteristics

	All	Response to TACE		<i>p</i> value	Association with TTP (<i>p</i> value)
		Responders(n=25)	Nonresponders(n=30)		
Age (years), mean ± SD	58±11	61±9	56±13	0.085	0.105
Male/female (n)	45/10	22/3	23/7	0.318	0.379
History of previous treatment, Y/N	3/52	2/23	1/29	0.585	0.670
Liver cirrhosis, Y/N	33/22	15/10	18/12	1.0	0.991
Hepatitis B virus, Y/N	41/14	15/10	26/4	0.032	0.416
Child-Pugh A/B (n)	32/23	18/7	14/16	0.098	0.163
BCLC stage A/B (n)	6/49	5/20	1/29	0.082	0.024
Pretreatment laboratory markers					
ALT > 50 U/L, Y/N	19/36	9/16	10/20	0.578	0.873
AST > 40 U/L, Y/N	38/17	15/10	23/7	0.244	0.822
ALP > 125 U/L, Y/N	21/34	4/21	17/13	0.002	0.002
GGT > 60 U/L, Y/N	41/14	16/9	25/5	0.127	0.323
INR > 1.2, Y/N	12/43	3/22	9/21	0.188	0.239
Bilirubin > 1.0 mg/dL, Y/N	16/39	5/20	11/19	0.237	0.043
Albumin < 35 g/L, Y/N	20/35	5/20	15/15	0.026	0.049
Creatinine > 1.5 mg/dL, Y/N	9/46	2/23	7/23	0.159	0.230
AFP > 20 ng/mL, Y/N	37/18	12/13	25/5	0.008	0.007
Tumour and therapy					
Number of HCCs				0.494	0.873
≥ 5	6	2	4		
< 5	49	23	26		
One	37	16	21		
Two	7	4	3		
Three	2	2	0		
Four	3	1	2		
Tumour size (cm), Mean±SD	7.90±4.42	4.91±2.28	10.39±4.24	<0.001	<0.001
No. of TACE sessions	2±1	2±1	2±1	0.057	0.046
Lesion distribution					
Unilobar (L/R/C)	43(8/34/1)	20(2/18/0)	23(6/16/1)		
Bilobar	12	5	7		

TTP time to progression, ALT alanine aminotransferase, AST aspartate aminotransferase, ALP alkaline phosphatase, GGT gamma-glutamyl transpeptidase, INR international normalised ratio, AFP alpha fetoprotein, SD standard deviation, L left lobe, R right lobe, C caudate lobe, Y yes, N no
 Bold type indicates when significance ($p < 0.05$)

between responders and non-responders to TACE in HCC patients. With multivariate analysis, we demonstrated that mRECIST assessment was associated with TTP independently, and that kurtosis of ADC_{total} had the best predictive performance for disease progression.

Previously retrospective studies concentrating on ADC measurement showed conflicting results for predicting response to TACE in patients with HCC. Mannelli et al. [18] found that HCCs with poor and incomplete response to TACE (< 50% necrosis on post-TACE MRI) had significantly lower pre-treatment ADC calculated by using 3 b values (0, 50 and 500 s/mm²). Likewise, Park et al. [7] found a higher pretreatment ADC value calculated by using b-values of 0, 25, 50, 75,

100, 200, 500 and 800 s/mm² in the lipiodol good uptake group than the lipiodol poor uptake group; however, there was no statistical difference between these two groups ($p = 0.073$). Furthermore, Dong et al. [19] found that the overall survival was significantly longer in the group with lower prechemoembolisation ADC calculated by using 2 b-value (0, 500 s/mm²) than in the group with higher ADC. In our prospective study, we strictly enrolled patients according to the inclusion criteria and ensured that regular follow-ups were conducted for an extended period of time without failure. Thus, we are confident in the homogeneity of our patients as far as staging and surveillance protocols are concerned with far more accurate TTP compared to other retrospective

Table 2 Differences in histogram metrics for intravoxel incoherent motion (IVIM) parameter maps between responders and non-responders

Parameters	D_{slow}		p value		D_{fast}		p value		PF		$ADC_{(0,500)}$		p value		ADC_{total}		p value	
	Responders (n=25)	Non-responders (n=30)	Responders (n=25)	Non-responders (n=30)	Responders (n=25)	Non-responders (n=30)	Responders (n=25)	Non-responders (n=30)	Responders (n=25)	Non-responders (n=30)	Responders (n=25)	Non-responders (n=30)	Responders (n=25)	Non-responders (n=30)	Responders (n=25)	Non-responders (n=30)		
Mean	1.13±0.19	1.07±0.10	0.113	53.31±20.50	50.11±12.81	0.502	16.82±5.47	13.90±2.94	0.022	1.53±0.18	1.33±0.16	<0.001	1.25±0.17	1.13±0.09	0.005			
Median	1.13±0.19	1.04±0.10	0.045	28.82±14.36	25.06±11.22	0.281	15.89±6.86	12.74±3.22	0.043	1.50±0.18	1.30±0.16	<0.001	1.21±0.17	1.11±0.09	0.008			
25 th percentile	0.99±0.17	0.93±0.10	0.078	11.73±9.69	10.50±4.06	0.806	11.33±5.14	6.59±3.26	<0.001	1.31±0.18	1.15±0.12	<0.001	1.09±0.16	1.01±0.12	0.039			
75 th percentile	1.26±0.22	1.18±0.12	0.117	69.18±35.98	65.61±26.86	0.675	23.53±8.55	19.27±4.43	0.031	1.73±0.25	1.52±0.17	0.001	1.33±0.19	1.25±0.11	0.086			
90 th percentile	1.40±0.27	1.34±0.14	0.286	136.24±56.82	132.07±35.86	0.752	30.28±9.34	26.73±5.86	0.092	1.94±0.29	1.82±0.24	0.102	1.46±0.23	1.41±0.14	0.353			
Standard deviation	0.21±0.09	0.21±0.05	0.851	61.01±19.73	62.04±11.70	0.819	10.48±3.88	9.96±2.19	0.560	0.33±0.08	0.38±0.09	0.049	0.18±0.08	0.21±0.06	0.121			
Skewness	0.28±0.81	0.65±0.84	0.098	2.26±1.02	2.32±0.79	0.809	0.51±0.62	1.08±0.61	0.001	0.76±1.37	1.16±0.79	0.180	0.59±0.75	0.61±0.95	0.927			
Kurtosis	4.26±1.89	5.94±6.19	0.230	10.21±8.19	9.83±5.87	0.906	4.08±3.02	5.54±3.09	0.005	4.09±1.37	6.68±4.21	0.005	4.32±2.18	6.94±3.07	0.001			

Data are expressed as means ± standard deviations

D_{slow} true diffusion coefficient ($\times 10^{-3} \text{ mm}^2/\text{s}$); D_{fast} pseudodiffusion coefficient ($\times 10^{-3} \text{ mm}^2/\text{s}$); PF perfusion fraction (%); $ADC_{(0,500)}$ apparent diffusion coefficient using 2 b-value ($\times 10^{-3} \text{ mm}^2/\text{s}$), ADC_{total} apparent diffusion coefficient using 12 b-value ($\times 10^{-3} \text{ mm}^2/\text{s}$)

Numbers for mean, median, standard deviation, 75th percentile, 90th percentile, and skewness of all parameters, 25th percentile of D_{slow} , PF, $ADC_{(0,500)}$ and ADC_{total} and kurtosis of ADC_{total} were compared for significance using Student's t test. Numbers for the rest of parameters were compared using a Mann-Whitney U-test

Bold type indicates significance ($p < 0.05$)

Table 3 Diagnostic performance of the valuable parameters for identifying responders and non-responders

Parameters	AUC (95% CI)	<i>p</i> value	Sensitivity (95% CI)	Specificity (95% CI)	PPV (95% CI)	NPV (95% CI)	Cutoff value
PF							
Mean	0.67 (0.53,0.79)	0.035	56.0 (34.9,75.6)	80.0 (61.4,92.3)	70.0 (45.7,88.1)	68.6 (50.7,83.1)	16.31
Median	0.67 (0.53,0.79)	0.026	44.0 (24.4,65.1)	93.3 (77.9,99.2)	84.6 (53.0,98.3)	66.7 (50.5,80.4)	16.90
25 th percentile	0.78 (0.65,0.88)	<0.001	68.0 (46.5,85.1)	80.0 (61.4,92.3)	73.9 (51.0,90.1)	75.0 (56.6,88.5)	8.72
Skewness	0.76 (0.63,0.87)	<0.001	88.0 (68.8,97.5)	63.3 (43.9,80.1)	66.7 (47.9,82.3)	86.4 (65.1,97.1)	0.95
Kurtosis	0.72 (0.58,0.83)	0.002	56.0 (34.9,75.6)	83.3 (65.3,94.4)	73.7 (48.8,90.9)	69.4 (51.9,83.7)	3.51
ADC_(0,500)							
Mean	0.80 (0.68,0.90)	<0.001	96.0 (79.6,99.9)	53.3 (34.3,71.7)	63.2 (46.0,78.2)	94.1 (71.3,99.9)	1.36
Median	0.79 (0.66,0.89)	<0.001	76.0 (54.9,90.6)	73.3 (54.1,87.7)	70.4 (49.8,86.2)	78.6 (58.6,91.9)	1.36
25 th percentile	0.78 (0.65,0.88)	<0.001	92.0 (74.0,99.0)	53.3 (34.3,71.7)	62.2 (44.8,77.5)	88.9 (64.4,98.7)	1.16
75 th percentile	0.75 (0.61,0.86)	<0.001	72.0 (50.6,87.9)	73.3 (54.1,87.7)	69.2 (48.2,85.7)	75.9 (56.1,89.9)	1.55
Kurtosis	0.72 (0.58,0.83)	0.001	48.0 (27.8,68.7)	86.7 (69.3,96.2)	75.0 (46.6,93.1)	66.7 (49.8,80.9)	3.67
ADC_{total}							
Mean	0.73 (0.59,0.84)	0.001	68.0 (46.5,85.1)	73.3 (54.1,87.7)	68.0 (46.5,85.1)	73.3 (53.7,87.9)	1.17
Median	0.72 (0.59,0.84)	0.002	60.0 (38.7,78.9)	83.3 (65.3,94.4)	75.0 (50.2,91.7)	71.4 (53.7,85.4)	1.18
25 th percentile	0.69 (0.55,0.81)	0.011	88.0 (68.8,97.5)	46.7 (28.3,65.7)	57.9 (40.6,73.9)	82.4 (56.6,96.2)	0.97
Kurtosis	0.82 (0.69,0.91)	<0.001	76.0 (54.9,90.6)	86.7 (69.3,96.2)	82.6 (60.6,95.2)	81.3 (63.6,92.8)	4.69

PF perfusion fraction (%), $ADC_{(0,500)}$ apparent diffusion coefficient using 2 b-value ($\times 10^{-3}$ mm²/s), ADC_{total} apparent diffusion coefficient using 12 b-value ($\times 10^{-3}$ mm²/s), AUC areas under the receiver operating characteristics curve, 95% CI 95% confidence intervals, PPV positive-predictive value, NPV negative-predictive value

Cut-off values were chosen to maximise the sum of sensitivity and specificity

Fig. 3 Receiver operating characteristic (ROC) curve and corresponding areas under the ROC curve (AUCs) of significant parameters for prediction of responders to transarterial chemoembolisation (TACE). Numbers in parentheses represent 95 % confidence intervals

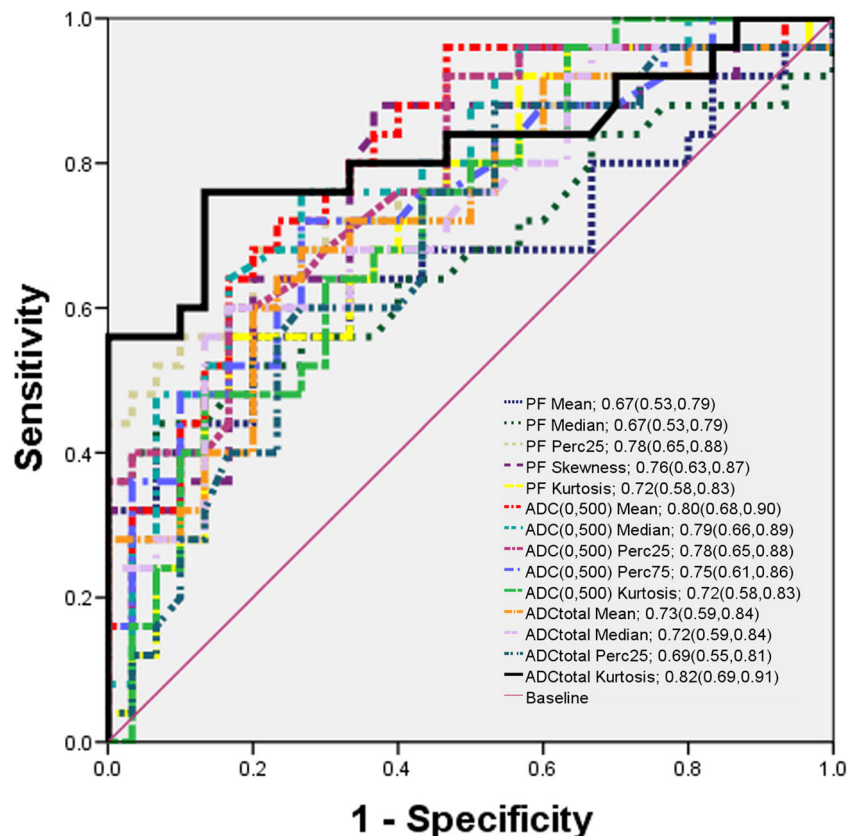


Table 4 Factors associated with time to progression (TTP) (n = 55)

Characteristic	Variable	Association with TTP (<i>p</i> Value)	
		Single-factor analysis	Multiple-factor analysis
mRECIST, R/Non	25/30	<0.001	<0.001
BCLC stage A/B	6/49	0.024	0.575
ALP>125 U/L, Y/N	21/34	0.002	0.431
Bilirubin > 1.0 mg/dL, Y/N	16/39	0.043	0.133
Albumin<35g/L, Y/N	20/35	0.049	0.130
AFP>20ng/mL, Y/N	37/18	0.007	0.065
Tumour size, L/M	32/23	<0.001	0.694
PF Median, L/M	41/14	0.035	0.390
PF 25 th percentile, L/M	31/24	0.002	0.383
PF Skewness, L/M	32/23	<0.001	0.816
PF Kurtosis, L/M	18/37	0.021	0.316
ADC _(0,500) Mean, L/M	17/38	<0.001	0.998
ADC _(0,500) 25 th percentile, L/M	17/38	0.001	0.635
ADC _(0,500) 75 th percentile, L/M	28/27	0.035	0.037
ADC _{total} Mean, L/M	29/26	0.005	0.324
ADC _{total} Median, L/M	33/22	0.032	0.667
ADC _{total} 25 th percentile, L/M	16/39	0.002	0.354
ADC _{total} Kurtosis, L/M	22/33	0.002	0.036

TTP time to progression, R responder, Non non-responder, ALP alkaline phosphatase, AFP alpha fetoprotein, Y yes, N no, L less than cutoff value, M more than cutoff value

Bold type indicates significance with multivariable analysis (*p* < 0.05)

studies. The mRECIST adopted in our study is the main form of assessing response to TACE for HCC based on the European Association for the Study of the Liver (EASL) and the AASLD [20, 21]. We also demonstrated that mRECIST was independently associated with TTP. Similarly, Gillmore et al. [16] have shown that overall responses measured by mRECIST between 2 and 3 months after the first TA(C)E are independently associated with 1-year survival. Moreover, in our study, parameters were derived from histogram analysis

of the entire lesion, while ADCs were derived from single slice-based regions of interest (ROIs) within tumours in their studies. The findings of our study showed that mean, median and 25th percentile of ADC_(0,500) and ADC_{total}, and 75th percentile of ADC_(0,500) were higher in responders compared with non-responders. We hypothesised that tumours with lower pre-TACE ADC may exhibit higher tumour cellularity and/or higher tumour grade, as shown in previously published papers [12, 22], which may lead to poor prognosis. In

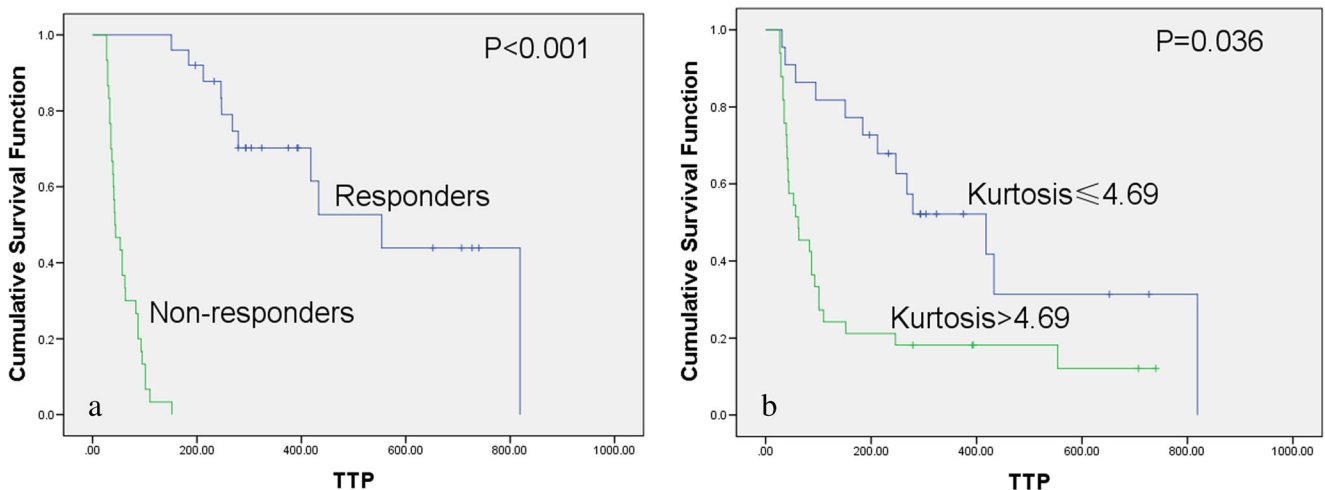


Fig. 4 Kaplan-Meier curves show comparison of time to progression (TTP) between responders and non-responders as assessed with mRECIST (a), kurtosis of ADC_{total} (b). *P* values are provided in the figure

Table 5 Independent factors for time to progression (TTP) with multiple-factor analysis

Factors	SE	Hazard ratio	95% CI
mRECIST criteria	1.362	642.088	44.486-9,267.550
ADC _(0,500) 75 th percentile	0.840	5.742	1.108-29.994
ADC _{total} kurtosis	0.631	0.266	0.077-0.915

SE standard error, 95% CI 95% confidence interval

addition, lower ADC may be secondary to reduced tumour perfusion, as ADC is a parameter contaminated by pseudo-diffusion [18].

By using IVIM with multiple b values and a bi-exponential model, a quantitative estimation for perfusion-sensitive parameters is generated. PF is defined as the fractional volume of capillary blood flowing in each imaging voxel [13, 23]. In our study, we found that the mean, median and 25th percentile of PF were higher in responders compared with non-responders. Woo et al. [22] found higher PF value in arterially hyperenhanced HCC. Chandarana et al [24] reported that the PF values of enhanced renal lesions were significantly higher compared with non-enhanced lesions ($p = 0.037$). As such, a low PF value may suggest slow movement or stagnant blood flow into capillaries of tumour, resulting in less chemoembolisation materials delivered to these areas. Likewise, Lewin et al. [25] put forward that increased PF values at 2 weeks in advanced HCC following sorafenib treatment is consistent with the effects of improved remaining vessels as well as basement membrane thickness and pericyte coverage. In this study, kurtosis of ADC_{total} was independently associated with TTP, and had the best discriminative performance. Kurtosis of ADC_{total} in non-responders was higher than in responders. Kurtosis reflects the peak and heaviness of the tails of ADC distribution values. A higher kurtosis value indicates more heterogeneous internal components and poorer cell differentiation [26–29]. HCC are known to exhibit substantial tumour heterogeneity, due to prolonged development of the disease. In a previous study [28], kurtosis of ADC values was also found to be higher in triple negative breast cancer (BC) that had significantly more recurrence events on multivariate analysis than in ER-positive subtype BC. Guan et al. [26] found that the normal cervix displays significantly lower ADC kurtosis than cervical cancer due to the homogeneity of normal tissues. Tumours with high heterogeneity generally have poorer prognoses, which may be secondary to a more aggressive biological or treatment resistance [30]. Identification of imaging features that correlate with TTP may potentially serve as a form of non-invasive prediction of TACE outcome and the decision of personalised treatment.

This study had several limitations that need to be acknowledged. Firstly, it was not possible to calculate correlations between different IVIM parameters and the pathology of

HCC in our study after treatment with TACE because none of the cases was sufficiently down-staged by local TACE for hepatectomy or liver transplantation. Secondly, the threshold values obtained in our study may be preliminary due to absent unification in using b values. However, adoption of a large number of b values including enough low b values that are less than 200 s/mm² enable precisely calculated perfusion-sensitive parameters and ADC_{total} to be obtained. Thirdly, with regard to patient baseline characteristics, there were statistical differences in hepatitis B virus, the serum level of ALP, albumin and AFP, and tumour size between responders and non-responders, which may potentially affect the patients' survival. Therefore, it is necessary to predict prognosis based on a combination of multiparametric imaging approach and individual clinical conditions.

In conclusion, we demonstrated that pre-TACE kurtosis of ADC_{total} can be used as the best independent predictor of subsequent responses to TACE.

Funding The authors state that this work has not received any funding.

Compliance with ethical standards

Guarantor The scientific guarantor of this publication is Mengsu Zeng.

Conflict of interest The authors of this manuscript declare no relationships with any companies whose products or services may be related to the subject matter of the article.

Statistics and biometry Shengxiang Rao kindly provided statistical advice for this manuscript.

Informed consent Written informed consent was obtained from all subjects (patients) in this study.

Ethical approval Institutional Review Board approval was obtained.

Methodology

- prospective
- diagnostic or prognostic study
- performed at one institution

References

1. Forner A, Llovet JM, Bruix J (2012) Hepatocellular carcinoma. *Lancet* 379:1245–1255
2. European Association for the Study of the Liver, European Organisation for Research and Treatment of Cancer (2012) EASL-EORTC clinical practice guidelines: management of hepatocellular carcinoma. *J Hepatol* 56:908–943
3. Reig M, Darnell A, Forner A, Rimola J, Ayuso C, Bruix J (2014) Systemic therapy for hepatocellular carcinoma: the issue of treatment stage migration and registration of progression using the BCLC-refined RECIST. *Semin Liver Dis* 34:444–455
4. Bruix J, Sherman M (2011) Management of hepatocellular carcinoma: an update. *Hepatology* 53:1020–1022

5. Wu L, Xu P, Rao S et al (2017) ADCtotal ratio and D ratio derived from intravoxel incoherent motion early after TACE are independent predictors for survival in hepatocellular carcinoma. *J Magn Reson Imaging* 46:820–830
6. Lin M, Tian MM, Zhang WP, Xu L, Jin P (2016) Predictive values of diffusion-weighted imaging and perfusion-weighted imaging in evaluating the efficacy of transcatheter arterial chemoembolization for hepatocellular carcinoma. *Onco Targets Ther* 9:7029–7037
7. Park YS, Lee CH, Kim JH et al (2014) Using intravoxel incoherent motion (IVIM) MR imaging to predict lipiodol uptake in patients with hepatocellular carcinoma following transcatheter arterial chemoembolization: a preliminary result. *Magn Reson Imaging* 32:638–646
8. Liang HY, Huang YQ, Yang ZX, Ying-Ding ZMS, Rao SX (2016) Potential of MR histogram analyses for prediction of response to chemotherapy in patients with colorectal hepatic metastases. *Eur Radiol* 26:2009–2018
9. Guo Y, Kong QC, Zhu YQ et al (2017) Whole-lesion histogram analysis of the apparent diffusion coefficient: Evaluation of the correlation with subtypes of mucinous breast carcinoma. *J Magn Reson Imaging* 47:391–400
10. Bougias H, Ghiatas A, Priovolos D, Veliou K, Christou A (2017) Whole-lesion histogram analysis metrics of the apparent diffusion coefficient as a marker of breast lesions characterization at 1.5 T. *Radiography (Lond)* 23:e41–e46
11. Donati OF, Mazaheri Y, Afaq A et al (2014) Prostate cancer aggressiveness: assessment with whole-lesion histogram analysis of the apparent diffusion coefficient. *Radiology* 271:143–152
12. Hu XX, Yang ZX, Liang HY et al (2017) Whole-tumor MRI histogram analyses of hepatocellular carcinoma: Correlations with Ki-67 labeling index. *J Magn Reson Imaging* 46:383–392
13. Yoon JH, Lee JM, Yu MH, Kiefer B, Han JK, Choi BI (2014) Evaluation of hepatic focal lesions using diffusion-weighted MR imaging: comparison of apparent diffusion coefficient and intravoxel incoherent motion-derived parameters. *J Magn Reson Imaging* 39:276–285
14. Makuuchi M, Kokudo N, Arii S et al (2008) Development of evidence-based clinical guidelines for the diagnosis and treatment of hepatocellular carcinoma in Japan. *Hepatol Res* 38:37–51
15. Nouse K, Tanaka H, Uematsu S et al (2008) Cost-effectiveness of the surveillance program of hepatocellular carcinoma depends on the medical circumstances. *J Gastroenterol Hepatol* 23:437–444
16. Gillmore R, Stuart S, Kirkwood A et al (2011) EASL and mRECIST responses are independent prognostic factors for survival in hepatocellular cancer patients treated with transarterial embolization. *J Hepatol* 55:1309–1316
17. Vandecaveye V, Michielsen K, De Keyzer F et al (2014) Chemoembolization for hepatocellular carcinoma: 1-month response determined with apparent diffusion coefficient is an independent predictor of outcome. *Radiology* 270:747–757
18. Mannelli L, Kim S, Hajdu CH, Babb JS, Taouli B (2013) Serial diffusion-weighted MRI in patients with hepatocellular carcinoma: Prediction and assessment of response to transarterial chemoembolization. Preliminary experience. *Eur J Radiol* 82: 577–582
19. Dong S, Ye XD, Yuan Z, Xu LC, Xiao XS (2012) Relationship of apparent diffusion coefficient to survival for patients with unresectable primary hepatocellular carcinoma after chemoembolization. *Eur J Radiol* 81:472–477
20. Lencioni R, Llovet JM (2010) Modified RECIST (mRECIST) assessment for hepatocellular carcinoma. *Semin Liver Dis* 30:52–60
21. Bruix J, Sherman M, Llovet JM et al (2001) Clinical management of hepatocellular carcinoma. Conclusions of the Barcelona-2000 EASL conference. European Association for the Study of the Liver. *J Hepatol* 35:421–430
22. Woo S, Lee JM, Yoon JH, Joo I, Han JK, Choi BI (2014) Intravoxel incoherent motion diffusion-weighted MR imaging of hepatocellular carcinoma: correlation with enhancement degree and histologic grade. *Radiology* 270:758–767
23. Ichikawa S, Motosugi U, Ichikawa T, Sano K, Morisaka H, Araki T (2013) Intravoxel incoherent motion imaging of focal hepatic lesions. *J Magn Reson Imaging* 37:1371–1376
24. Chandarana H, Lee VS, Hecht E, Taouli B, Sigmund EE (2011) Comparison of biexponential and monoexponential model of diffusion weighted imaging in evaluation of renal lesions: preliminary experience. *Invest Radiol* 46:285–291
25. Lewin M, Fartoux L, Vignaud A, Arrive L, Menu Y, Rosmorduc O (2011) The diffusion-weighted imaging perfusion fraction f is a potential marker of sorafenib treatment in advanced hepatocellular carcinoma: a pilot study. *Eur Radiol* 21:281–290
26. Guan Y, Shi H, Chen Y et al (2016) Whole-Lesion Histogram Analysis of Apparent Diffusion Coefficient for the Assessment of Cervical Cancer. *J Comput Assist Tomogr* 40:212–217
27. Zhang Y, Chen J, Liu S et al (2017) Assessment of histological differentiation in gastric cancers using whole-volume histogram analysis of apparent diffusion coefficient maps. *J Magn Reson Imaging* 45:440–449
28. Choi Y, Kim SH, Youn IK, Kang BJ, Park WC, Lee A (2017) Rim sign and histogram analysis of apparent diffusion coefficient values on diffusion-weighted MRI in triple-negative breast cancer: Comparison with ER-positive subtype. *PLoS One* 12:e177903
29. Yoon SH, Park CM, Park SJ, Yoon JH, Hahn S, Goo JM (2016) Tumor Heterogeneity in Lung Cancer: Assessment with Dynamic Contrast-enhanced MR Imaging. *Radiology* 280:940–948
30. Davnall F, Yip CS, Ljungqvist G et al (2012) Assessment of tumor heterogeneity: an emerging imaging tool for clinical practice? *Insights Imaging* 3:573–589